Cohesion and lattice stabilities in the 5*d* transition metals: Full versus muffin-tin potentials

G. W. Fernando, R. E. Watson, M. Weinert, Y. J. Wang, and J. W. Davenport
Department of Physics, Brookhaven National Laboratory, Upton, New York 11973-5000
(Received 13 October 1989)

First-principles linear augmented-Slater-type-orbital (LASTO) calculations have been carried out for the 5*d* transition metals Hf through Au. Among the various topics discussed are the stability of the hcp, fcc, and bcc phases, lattice volumes, and cohesion. Effects of the full versus the muffin-tin potential are also examined; in particular the ground state of Au is now correctly predicted to be fcc with use of the full potential. The hcp-fcc energy differences are a factor of 5 smaller than the corresponding fcc-bcc energy differences along the row.

I. INTRODUCTION

It is now common practice for first-principles electronic-structure calculations, based on the local-density approximation (LDA), to yield the total energy of the system for which the calculation was done. This, then, allows the exploration of the relative stabilities of different phases, including metastable phases which may be inaccessible experimentally. Normally one takes differences of total energies, as in the case of the heat of formation of a compound where the difference is between the calculated total energy of the compound and those of the elemental reference materials. Experience[1] shows that accurate heats of formation are obtained when both the compound and the reference systems are well-packed structures for then the total energies are obtained to a common accuracy (or error). The situation is quite different when dealing with the cohesive energy of an elemental solid where the energy difference is between the solid and the free atom. It appears that the local-density approximation does a poorer job on the free atom (i.e., the calculated heats are too large) in part because of the LDA's inadequate treatment of multiplet effects. Recently the full-potential scheme has been incorporated[2] into our linear augmented-Slater-type-orbital (LASTO) method and this will be used to peruse full potential estimates of the cohesive energies across the 5*d* transition-metal row. To our knowledge this is the first time that such a sequence has been dealt with in the full-potential scheme. There are several ways in which one can attempt to account for multiplet effects when applying local-density theory to the total energy of an atom (the simplest one being to ignore them), and the consequences of these choices on the resulting calculated cohesive energy of the solid will be inspected. Also, there has been a long-standing controversy[3,4] over the relative stabilities of the elemental transition metals in the bcc, versus the fcc, versus the hcp structures. These stability energies enter phase diagram constructs: for the most part they are not directly accessible from experiment and for 25 years band theory has yielded[3] values which are not convenient to phase-diagram constructs as they are normally done. This issue is revisted here with full-potential calculations, and while the results do not differ significantly from earlier results,[5,6] there does appear to be some agreement between the predictions for the fcc-bcc energy differences and what phase-diagram constructs can live with.[4] Some essential disagreements remain for the fcc-hcp lattice stabilities.

The LASTO scheme[7] employs Slater-type orbitals as a basis set in the interstitial region between atoms and augments these with explicit solutions of the single-particle equation within nonoverlapping atomic spheres centered on the atomic sites. The full-potential version[2] of the scheme employs aspherical terms in the potential both within and outside the spheres. "Muffin-tin"–potential results will also be reported where only spherical terms are kept inside the spheres and a constant potential is used outside. Some results will be reported where a single *s*, *p*, and *d* Slater orbital is used per atomic site, resulting in a 9×9 matrix to be diagonalized that is not only small, but also has the structure of a tight-binding matrix (from which tight-binding matrix elements might be derived). Larger, "double-ξ" basis sets have also been used where two *s*, two *p*, two *d*, and a single *f*-like "polarization" Slater orbital(s) are used. The resulting total energies are in essential agreement with linear augmented-plane-wave (LAPW) calculations with their much larger basis sets and larger matrices to diagonalize. The double-ξ basis-set calculations are measurably more costly in computer time than the single-ξ results and we will compare total-energy results obtained with the two sets. LASTO depends on a choice of basis sets; this choice and some other features of the calculations are described in the Appendix.

The plan of the paper is as follows. Total energies are obtained for the 5*d* elemental metals Hf through Au and the effects of going from single to double basis set and from muffin tin to full potential are considered in Sec. II. This is followed by estimates of the lattice stabilities, which are seen to be little affected by going to larger basis sets or more rigorous potentials since the total energies for each of the two structures involved benefit similarly from the improved calculations. When considering the

hcp lattice stabilities it is necessary to treat their c/a ratios variationally: while the calculated c/a are in reasonable accord with experiment for those systems which form in the hcp structure, quite different c/a are obtained for some of the other metals and the changes in total energies associated with these differences are significant. Calculated bulk moduli and variationally determined lattice volumes are reported for several of the metals in Sec. IV and this is followed by inspection of the full potential obtained for different directions in the crystal for hcp Os (similar results were reported previously[2] for bcc W and fcc Pt). The potential for this metal at the observed c/a ratio will be compared with that of the ideal c/a and this, in turn, with fcc Os. Finally the cohesive energies are calculated using local-spin-density approximation[8] (LSDA) calculations to estimate the reference energy in the free atom for state of maximum spin multiplicity for some given atomic configuration. It has been traditional to take the result of lowest energy, to declare this the ground-state configuration of the atom within the local-density approximation, and to use this as the reference energy in

$$E_{\text{coh}} \equiv E(\text{metal}) - E(\text{free atom}) \tag{1}$$

to estimate cohesion. This will be done here. The problem is that this does not correspond to the experimental situation where cohesion is measured with respect to the atom in its ground state since the LSDA result usually involves an *average* over a set of multiplet levels of some given spin. One can use the experimental atomic spectra to estimate the promotion energy from the atom's ground state to this average for different atomic configurations, e.g., d^n, $d^{n-1}s$, $d^{n-2}s^2$, etc. In all cases the cohesive energy is overestimated, thus implying local-density theory does better for the solid than the free atom.

II. THE EFFECTS OF BASIS-SET SIZE AND CHOICE OF POTENTIAL

Figure 1 displays the changes in total energy (1) upon going from the double basis set (with f-like polarization term) with full potential to the single s, p plus d basis also with full potential (the circles), and (2) taking the single basis set, in turn, to calculations with a muffin-tin potential (the solid squares). The zero of the plot then corresponds to the total energies of the double set with full potential. It should be noted that these energies range from $\sim 5\times 10^5$ eV/atom for the lighter elements to $\sim 10^6$ eV/atom for the heavier elements. The improvements associated with either full potential or better basis set, while tiny on the scale of the overall energy, are nevertheless significant on the scale of binding energies. The systems of concern here are well packed, with high site symmetries, and the effect of going from the muffin tin to the full potential should be measurably greater in ill-packed systems such as occur for a few of the elements (e.g., As) and for many compounds.

From Fig. 1 the full potential is seen to be most important for describing elements in the middle of the transition-metal series. Naively one expects the maximum effect at half-filling of the d bands, i.e., W. To rationalize the pronounced shift of the maximum towards Os, we consider the nonspherical components of the Coulomb full potential at the sphere boundaries, $V_{l_v}(R)$. Since the sphere volumes have been chosen to be a constant fraction of the unit-cell volume across the row, we must scale $V_{l_v}(R)$ to account for variations in volume among the elements. (The bare numbers for Hf, Ta, . . . , are comparable to Os.) Scaling $V_{l_v}(R)$ by $R^{-(l_v+1)}$ — which can be argued is an appropriate scaling for the contribution to the total energy assuming an approximately constant interstitial charge—will have a much larger relative effect for Hf than Os. The total-energy differences between the muffin-tin and full-potential results of Fig. 1 and $R^{-(l_v+1)}V_{l_v}(R)$ for the bcc ($l_v=4$), fcc ($l_v=4$), and hcp ($l_v=5$) structures are shown in Fig. 2. We have normalized all the values to those for Os. The correlation of these quantities is surprisingly good. Figure 2 suggests that the small volume of Os (Os has the smallest atomic volume in the 5d row) has a direct influence on the nonspherical contributions to the total energy. Smaller atomic volumes will have several direct effects: the interatomic (Madelung) potential, which scales as the inverse of the lattice constant, is larger; likewise, the tails of states centered on one site will have larger nonspherical contributions on neighboring sites resulting in larger nonspherical contributions to the total energy.

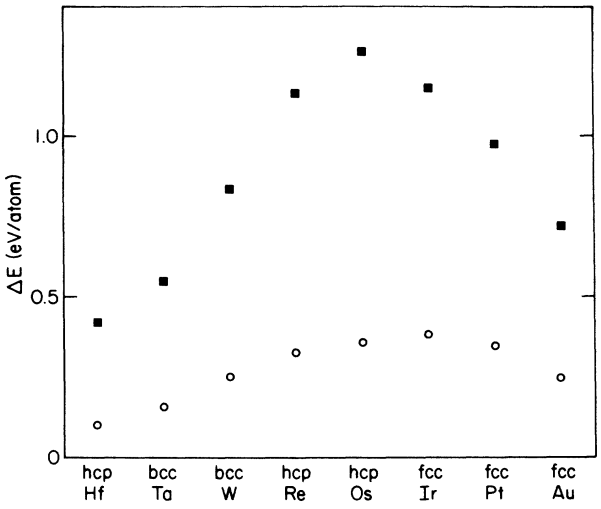

FIG. 1. Differences in crystal total energies for the elemental 5d metals at their observed lattice constants. The zero, with respect to which the other energies are measured, is the total energy of the calculation employing the full-potential and the double Slater-type orbital (STO) basis set. The open circles are the energies of the full-potential single STO calculations measured with respect to the double set energies, while the squares are the result of employing muffin-tin potentials and the single STO.

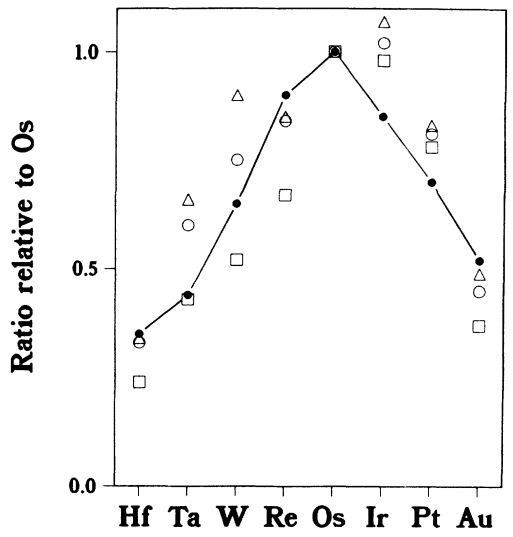

FIG. 2. Total-energy differences between the muffin-tin and full-potential results of Fig. 1 (—·—·—·) and the nonspherical component of the Coulomb potential on the muffin-tin sphere of radius R divided by R^{l_v+1} for the bcc ($l_v=4$; ○), fcc ($l_v=4$; □), and hcp ($l_v=5$; △) structures. All values are normalized to unity at Os.

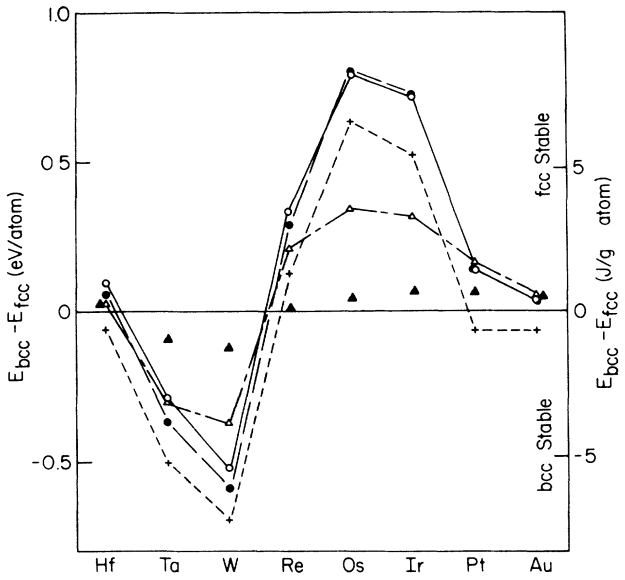

FIG. 3. fcc-bcc energy differences calculated (i) with full potential and double STO (open circles), (ii) with full potential and single STO (solid circles), and (iii) with muffin-tin potentials and single STO (+ symbols). The solid triangles are Kaufman's estimates (Refs. 3 and 9) and the open triangles are the estimates of Saunders *et al.* (Ref. 4) of these promotion energies.

III. LATTICE STABILITIES

As has already been noted, the relative stabilities of the elemental solids in the fcc versus bcc versus hcp structures enter phase-diagram constructs. Consider bcc Mo alloyed with fcc Ir: there is a bcc phase with dilute Ir alloyed into bcc Mo and the leading energy term is taken to be the energy to promote Ir from the fcc to the bcc structure (and not to embed Ir in bcc Mo). Similarly there is a terminal Ir-based phase involving promoting Mo to the fcc structure. Also, at intermediate concentrations the *d* bands are, *on average,* filled to a point where the elemental transition metals have the hcp structure, and at these concentrations Mo-Ir displays a hcp solution phase. Part of the energetics associated with this phase is taken to be the energy necessary to promote Mo and Ir separately to the hcp structure. Kaufman, using what thermodynamic data were available, made the pioneering estimates[3,9] of these promotion energies, which for years have been employed in phase-diagram constructs. Despite the lack of any good band-theory estimates, Mott and Friedel argued[3] 25 years ago that Kaufman's values were much smaller in magnitude than what band theory would yield. This is illustrated in Fig. 3, where our current estimates of the fcc-bcc energy differences are shown and compared with Kaufman's estimates (the solid triangles). There is disagreement by an order of magnitude between his values and the present results.

The two sets of full-potential results, with the single and double basis sets, are essentially identical, while the muffin-tin values lie below them. The muffin-tin results are of the wrong sign for Pt and Au, which are fcc metals, and the result for Hf (an hcp metal) is arguably wrong. It is to be noted that the calculations done here were done with a common-sized sphere for the different structures of a given metal (see the Appendix), although the fcc lattice will accommodate larger nonoverlapping spheres than will a bcc lattice of equal atomic volume. If muffin-tin calculations are done with touching atomic spheres for both structures, i.e., larger ones for the fcc, then the muffin-tin results shift upwards, are of the correct sign for Hf, Pt, and Au, and are in good agreement with the full-potential results.

The remaining, open-triangle curve of Fig. 3 is based on recent estimates[4] by Saunders *et al.* They took the available thermodynamic data and asked how far the lattice-stability results could be pushed towards an *a priori* theory without being inconsistent with the thermodynamic data, including the phase diagrams. Except for Os and Ir there is accord between their results and the full-potential band-theory estimates.

The situation is different for the fcc-hcp energy differences, as is to be seen in Fig. 4. Note that these energy differences are typically a factor of 5 smaller than was the case in Fig. 3. The smaller fcc-hcp energy differences follow from the fact that the twelvefold nearest-neighbor atomic positions are essentially the same in the two structures. Here the muffin-tin and full-potential results are in essential agreement.

The problem between the *a priori* calculations and the phase-diagram estimates occurs with the sign of the lattice term for Ta and W (and for V, Cr, Nb, and Mo which reside in the same columns of the Periodic Table). If fcc Ta is to be stabler than its hcp counterpart, as the band-theory calculations indicate, then there are problems modeling intermediate hcp phases, as is currently done, when bcc metals, such as Mo or Ta, are alloyed with the heavy fcc transition metals, such as Ir or Pd.

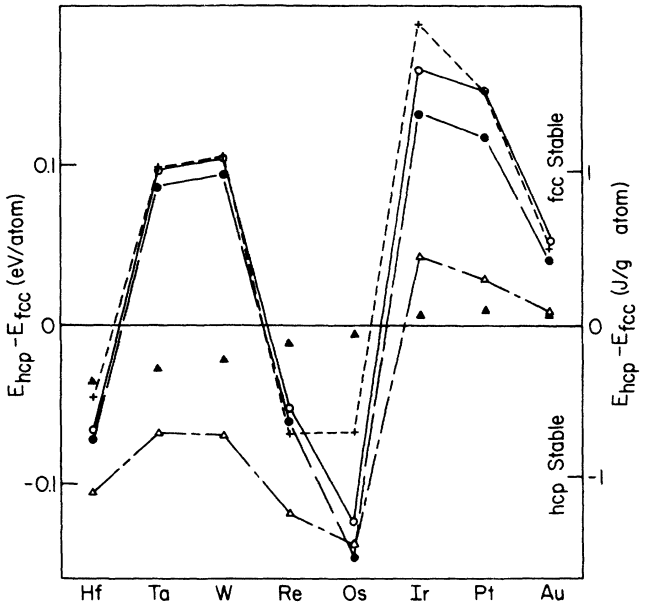

FIG. 4. fcc-hcp energy differences: see Fig. 3 for the notation. Note the different energy scales of this and of Fig. 3.

The only case of accord between our (and earlier) results and those of Saunders *et al.* occurs for Os. Our results are in accord with experiment: the fcc metals are calculated to have the fcc phase stable and similarly the hcp metals are predicted to be hcp. The problem remains with the bcc metals. Are the hcp or fcc the stabler among the metastable phases?

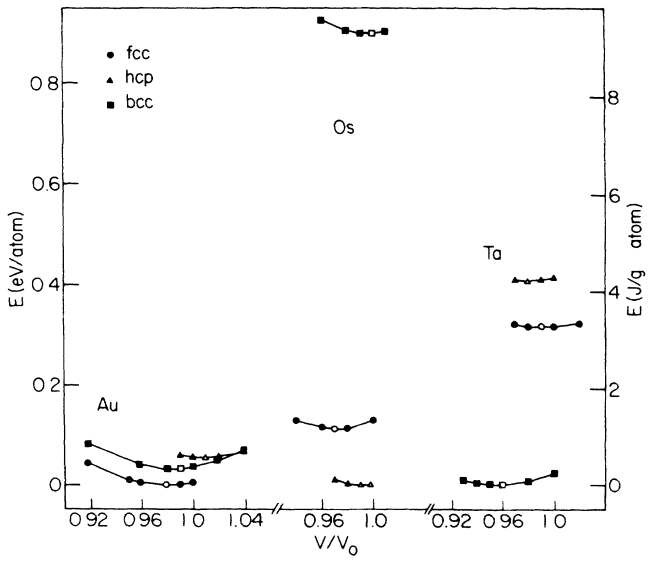

FIG. 5. Full-potential, double-basis-set energies of Au, Os, and Ta, in the bcc, fcc, and hcp phases, as a function of atomic volume measured with respect to the observe volume V_0. Open symbols indicate the lowest-lying point on any curve, and the zero, for each element, has been taken to be its lowest calculated total energy.

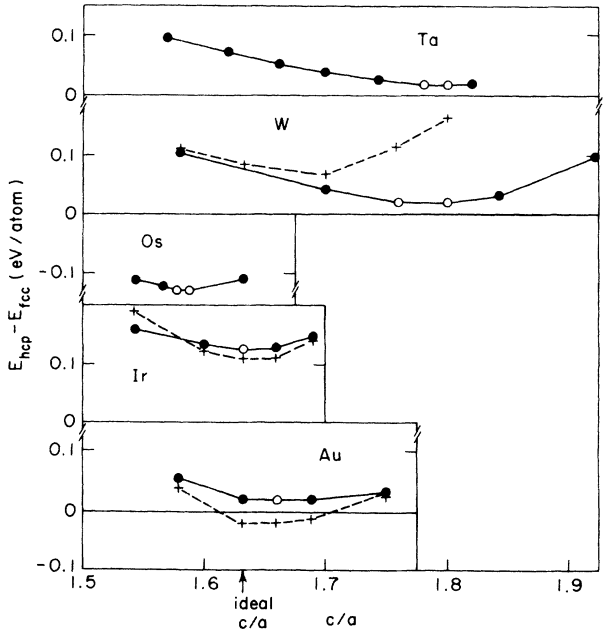

FIG. 6. hcp-fcc energy differences for Ta, W, Os, Ir, and Au as a function of the hcp c/a ratio employed in the calculation. The circles are full-potential, double-basis-set results, while the + symbols indicate muffin-tin single-STO results. The open circles indicate the lowest-lying points on the curves.

The calculations of Figs. 1, 3, and 4 employed the observed atomic volumes and for hcp Hf, Re, and Os the observed c/a ratios of 1.58, 1.61, and 1.58, respectively. These c/a ratios are almost the same and this provided the basis of choice for the c/a value in calculations where the other metals were taken to be hcp. This raises the question of what effect these choices have had on the computed lattice stabilities. The total energies, measured with respect to the lowest calculated energy, are plotted for Au, Os, and Ta in Fig. 5 as a function of atomic volume. The open symbols denote the lowest energy on any given curve. Going to the variationally determined minima has almost a zero effect on the calculated lattice stabilities. The situation is quite different when it comes to the c/a ratios. The full-potential, double-basis-set hcp-fcc lattice stabilities are plotted in Fig. 6 for Ta, W, Os, Ir, and Au, as a function of assumed hcp c/a value. Os is the one hcp metal and the variationally determined c/a is in accord with its observed value of 1.58. However, the metastable hcp phases of the other four metals have optimum c/a that deviate in varying degree from this. The minima for W and Ta are for c/a well above the ideal value although less than the observed c/a of such hcp metals as Zn and Cd. Going to the optimized c/a for Ta and W brings these lattice stabilities much closer to zero *but does not change their sign.* Muffin-tin results (the + symbols) are also shown for several of the metals in Fig. 6. These are not always in accord with the full-potential results and, perhaps most notably, one has hcp Au more stable than the fcc in such a description.

The effect on the hcp-fcc lattice stabilities on going from "typical" c/a values to variationally determined

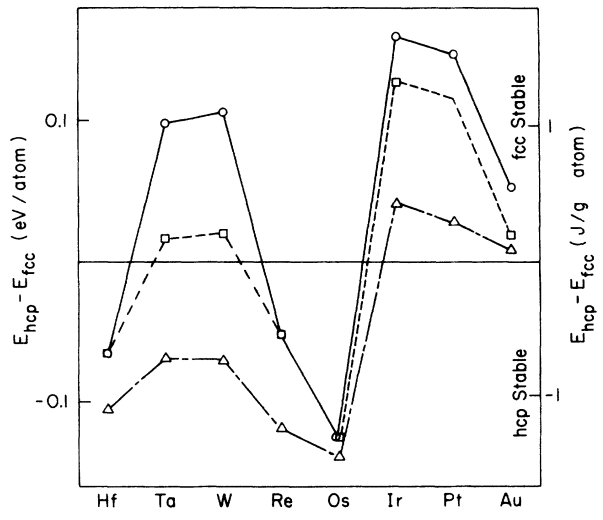

FIG. 7. Full-potential double-basis-set results for the lattice stability, $E_{hcp} - E_{fcc}$, assuming typical transition-metal c/a ratios as were used in Fig. 4 (open circles) and using the variationally determined c/a ratios of Fig. 6 (open squares and dashed line): values for Hf, Re, and Pt on this latter curve were simply sketched in, based with an eye toward the other results. The open triangles are the results of Saunders *et al.* (Ref. 4).

ones is summarized in Fig. 7 for calculations employing the full potentials and double basis sets. It appears unlikely that any further refinement of calculations, done within the local-density approximation, will lead to a reversal in sign for the W and Ta stabilities. The disagreement on this issue with Saunders *et al.*[4] remains.

IV. LATTICE VOLUMES AND BULK MODULI

The correct crystal structures lie lowest in Fig. 5 and the lattice volumes, obtained variationally for these structures, are in reasonable accord with experiment. The calculated volumes are smaller by 1%, 2%, and 4% for Os, Au, and Ta, respectively. Generally the calculated volumes for the metastable phases are also smaller than the volumes observed for the stable phase by a few percent, though this is not the case for hcp Au and bcc Os.

Calculated bulk moduli are tabulated in Table I and are in accord with experiment for Ta and Os while in but fair agreement for Au. The recent calculations[10] of Takeuchi, Chan, and Ho for Au, employing norm-conserving pseudopotentials, yield a more accurate bulk modulus and a lattice volume which is also within about 2% of experiment. However, as will be seen in Sec. VI, they do more poorly with the cohesive energy.

TABLE I. Comparison between calculated and experimental bulk moduli for Ta, Os, and Au.

	Present calc. (Mbar)	Calc.[a] (Mbar)	Expt. (Mbar)
Ta	2.0		2.0
Os	4.0		4.2
Au	2.3	1.79	1.7

[a]Reference 10.

V. THE FULL POTENTIALS: hcp Os

Os and Ir are the two heaviest known elements and hence hcp Os is one of the most closely packed elemental solids. The observed phase of hcp Os has a smaller c/a ratio compared to the ideal one. Here we will consider both the ideal and the observed hcp Os.

The full potentials, plotted for different directions off of the atomic site, are shown for hcp Os with the ideal c/a ratio in Fig. 8. The different directions are indicated in the inset in the figure. Most notable is the fact that the potential differs by as much as 10 eV for different parts of the interstitial region with the potential along the nearest-neighbor line lying markedly lowest. Compare Fig. 8 with Fig. 9, a plot of the potential along the equivalent four directions for Os in the fcc structure. These potentials look remarkably similar (to within a few tenths of a volt) between fcc and hcp phases along these four directions. This is not a surprising result since the two phases closely resemble one another (they have identical nearest neighbors); however, it is an interesting one since to our knowledge this has not been demonstrated quantitatively as is done here.

Directions (a) and (b) (Fig. 8) for the ideal c/a hcp case indicate the difference between *having* an occupied site above, i.e., along the c axis, and *not having* an occupied site above. On the (0001) plane, this difference is not significant.

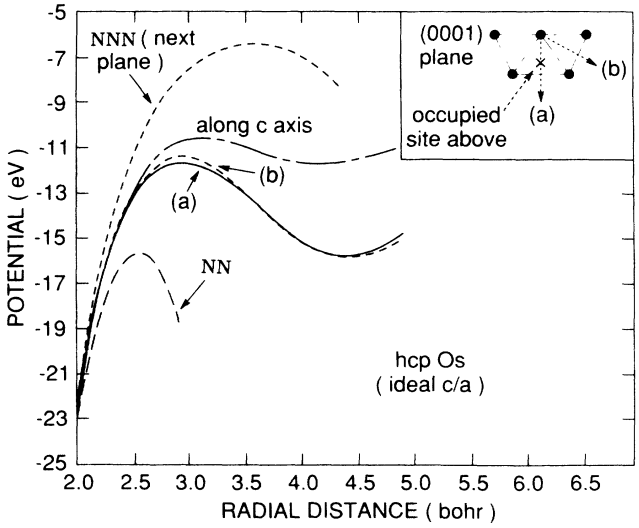

FIG. 8. Actual full crystal potential (double-basis-set run) plotted, for hcp Os with the ideal c/a ratio, along the crystal directions indicated. These have been shown up to slightly beyond the halfway point between neighboring atoms along a specified direction. The nearest-neighbor (NN) potential is the deepest and shows variations of the order of 5 eV in the interstitial compared to the potentials in other directions.

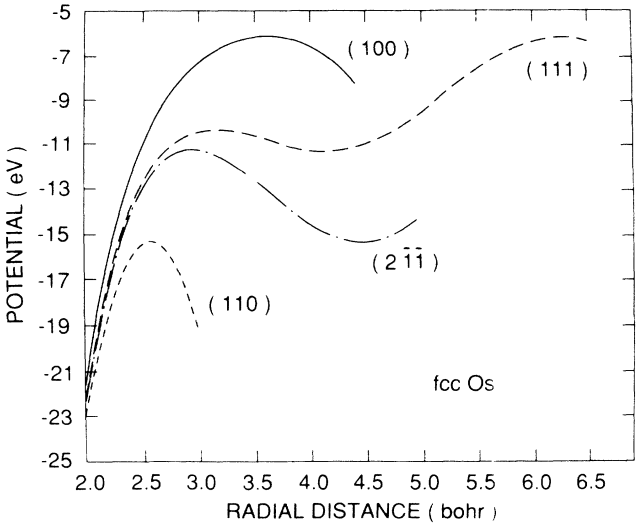

FIG. 9. Actual full crystal potential plotted, for fcc Os at the observed hcp atomic volume, along the crystal directions indicated. These have been shown up to slightly beyond the halfway point between neighboring atoms along a specified direction. When these potentials are compared with those in Fig. 8, it is clear that they are very similar for the equivalent directions. The only major difference is along the [111] direction, which has a double-minimum structure in the fcc case before running into the neighboring atom. In the hcp case there is only a single minimum due to its different stacking.

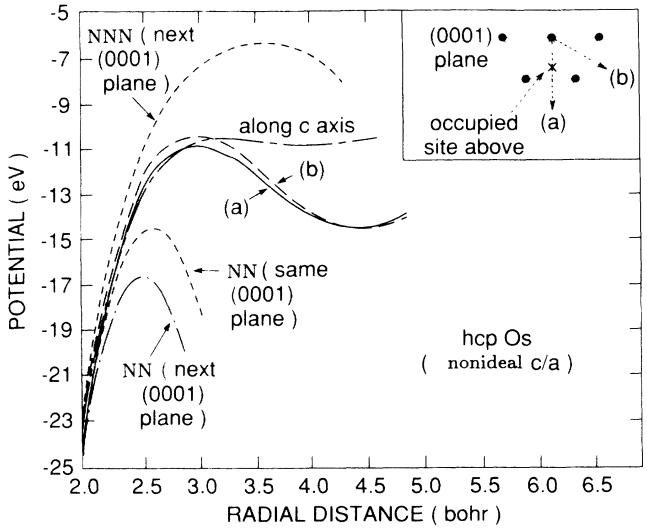

FIG. 10. Actual full crystal potential plotted for hcp Os with the observed lattice constants, along the directions indicated with the potential along the nearest-neighbor line now split since the ideal hcp nearest neighbors are no longer at a common distance due to the nonideal c/a ratio. The observed c/a is less than the ideal ratio (see Fig. 6) and hence the nearest-neighbor (NN) direction to the next (0001) plane produces the deepest potential. The splitting in the NN potential is about 2 eV in the interstitial due to about an 3% decrease in the c/a ratio.

Along the [111] direction in the fcc case (Fig. 9) there is, as was discussed previously,[2] a double-well potential with minima at the empty $\frac{1}{3}$ sites, while along the corresponding z direction in the hcp case (Fig. 8) there is only a single minimum. This is because the $\frac{2}{3}$ site (in the previous fcc notation) is occupied in the hcp case. Now compare the ideal c/a results with those for the observed c/a shown in Fig. 10. The nearest-neighbor (NN) potential is split in the nonideal hcp case. The direction of the splitting depends on whether the neighbor in question lies on the same (0001) plane or on the next plane. The magnitude of the splitting near the sphere boundaries is about 2 eV which is due to an about 3% decrease in the c/a ratio. The deepest potential well shown here (in Figs. 8–10) is along (a) or (b) in the hcp case and along the equivalent [2 1̄ 1̄] direction in the fcc case. However, note that this is actually a saddle point with a steep maximum in the [110] direction occurring exactly at this point.

In fact, *all* the minima shown here in the interstitial region are actually saddle-point structures. For example, the location of the minimum seen along the [111] (Fig. 8) direction exactly corresponds to the location of the maximum seen along the [2 1̄ 1̄] direction.

Also note that the potentials along various directions show differences of about 5–10 eV in the interstitial region, again showing that a simple muffin-tin potential may not be sufficient to describe subtle aspects of these phases. The successes of the muffin-tin potentials are surprising in view of this.

Individual harmonic terms, ρ_{l_v}, of the hcp Os charge density are displayed in Fig. 11. The most striking feature here is that it is the $l_v=5$ component, which turns out to be the largest in the 5d metals Os. Such a component involves wave-function character of higher l than that due to s, p, or d bands. Charge tails coming from adjacent atomic sites are responsible for ρ_5. Since the charge density ρ is obtained by taking the product $\psi^*\psi$, it is clear that the crystal wave function ψ must be

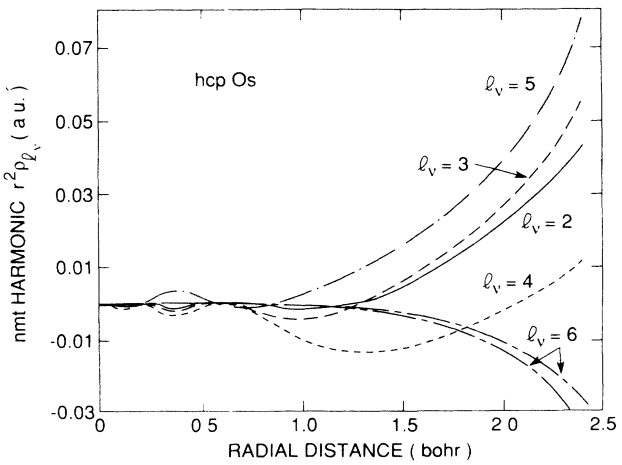

FIG. 11. Higher ($l_v=2$, 3, 4, 5, and 6) harmonics of the electron density in hcp Os. Note that the $l_v=5$ term turns out to be the largest near the sphere boundary, indicating tailing effects from other sites. Also, the nodal structure of, say, ρ_4, resembles that of a 5d function inside the sphere.

expanded up to at least $l=3$ in order to reasonably represent the charge density. The nodal structure of the density terms at the smaller radii reflects their atomic character as discussed previously[2], e.g., the $l_v=4$ density term has the nodes of the $5d$ wave function (e.g., it has two nodes). However, near the sphere boundary there are obvious deviations from the above-mentioned atomic-like behavior, indicating the importance of higher-l terms as observed in the previous paper.[2] We also find that the $l_v=7,8$ terms (not shown) are at least a factor of 3 or 4 smaller than the smallest harmonic shown here, indicating the adequency of our l expansion, which has a cutoff of $l_{\max}=8$ for the wave functions.

VI. COHESION

Cohesive energies involve the difference in energy between the crystal and free atom. As already was discussed in Sec. I, one may simply take a LSDA result for the free atom, obtained for that atomic configuration having the lowest LSDA total energy, and subtract that from the crystal total energy. However, the LSDA result for the free atom corresponds to an average over a set of spin multiplet levels for a given atomic configuration. It is possible to use spectroscopic data to correct the free atom's total energy for the energy cost associated with going from the free-atom ground state to the multiplet level average corresponding to the LSDA calculation. For example, the atomic configuration $5d^8 6s$ of Ir has two quartets, ^4F and ^4P, both of which will be used in a LSDA average. It can be seen from spectroscopic data that the average energy of these lies 1.14 eV above the lowest-lying multiplet level (ground state) of the atom.

The simple LSDA result and the results of correcting $5d^{n-1}6s$ LSDA energies for the promotion energy are shown in Fig. 12, where the full-potential, double-basis-set calculations were employed for the crystal energies. The present results for W agree to within a few hundredths of an eV/atom with the FLAPW results of Jansen and Freeman[11] and of Mattheiss and Hamann.[12] Accounting for promotion-energy effects measurably improves the agreement with experiment, and while the calculations consistently overestimate the cohesive energies, fair agreement with experiment is obtained for Hf, Ta, and Au. The effects of going to the single basis set or to the muffin-tin potential can be obtained by subtracting the results of Fig. 1 from the cohesive energies of Fig. 12. Going to the muffin-tin results would greatly improve the numerical agreement with the experimental cohesive energies at the middle of the row (while worsening the agreement for Hf, Ta, and Au)—of course, by introducing errors to compensate for the errors already in the estimates of ΔE_{coh}.

There are spectroscopic data[13] for atomic configurations other than the $5d^{n-1}6s$, allowing estimates to be made for other promotion-corrected ΔE_{coh}. Some of those cases, for which there are sufficient data, are collected in Fig. 13. The downwards arrows on some of the points indicate cases where the spectroscopic data are incomplete, i.e., some of the multiplet levels necessary for the averaging have not been observed. These are normally the higher lying of these levels and, thus, the resulting estimates are upper bounds on the values of ΔE_{coh}. As seen by the cases plotted, there are substantial data across the row for the d^{n-2} and $d^{n-2}sp$, but only sparse results for d^n, $d^{n-1}p$, and $d^{n-1}6d$. None of these cases yield results in better agreement with experiment than those already obtained with the $d^{n-1}s$.

The $d^{n-2}s^2$ values lie consistently above the $d^{n-1}s$. This implies that the experimental atomic $s \rightarrow d$ promotion or transfer energy

$$\Delta_{s\rightarrow d} \equiv E(d^{n-1}s) - E(d^{n-2}s^2)$$

is greater, i.e., more positive, than the calculated LSDA result. Gunnarsson and Jones observed[14] this tendency in the $3d$ row, from which they inferred that the atomic calculations overestimate the stability of the $d^{n-1}s$ with respect to the $d^{n-2}s^2$. Gunnarsson and Jones argued that this arose from a discrepancy in how local-density theory deals with the exchange interaction of a valence d electron, versus a valence s, with the atomic core. If this were the case one would expect the same trend to hold

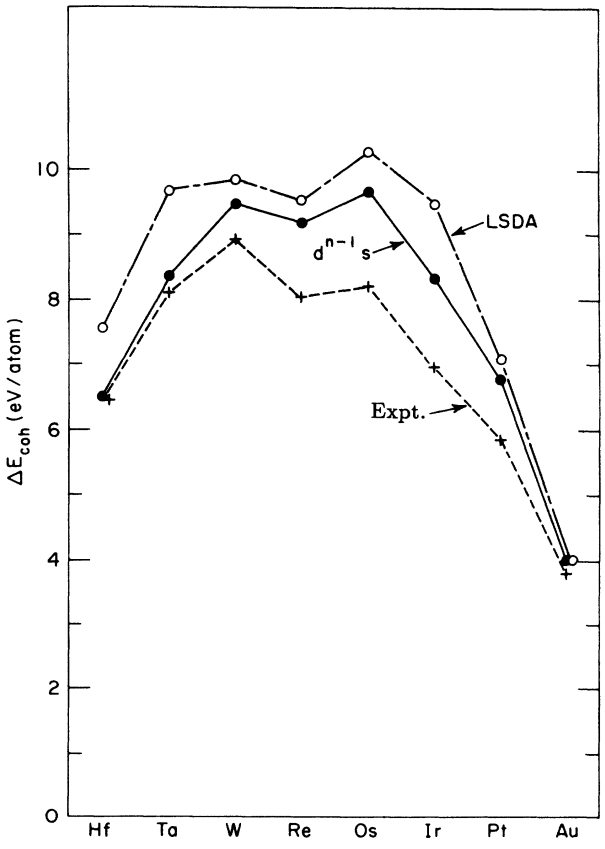

FIG. 12. Cohesive energies of the $5d$ transition metals, with their observed structures and lattice constants as obtained (i) with the LSDA approximation (ignoring multiplet promotion energies in the free atoms), and (ii) where the $d^{n-1}s$ LSDA free atom has been used and the promotion energy from the free-atom ground state to the center of the calculated LSDA level has been estimated from free-atom spectroscopic data.

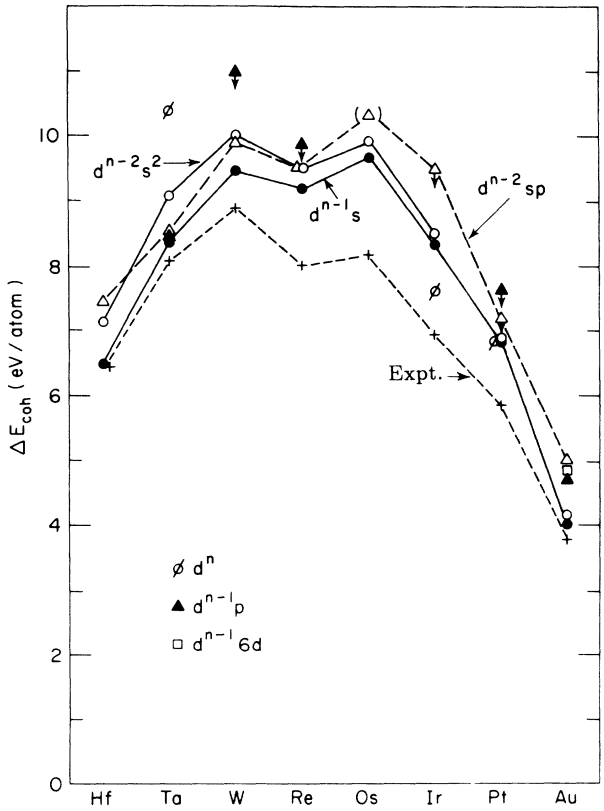

FIG. 13. Cohesive energies of the 5*d* transition metals employing LSDA calculations for various free-atom configurations, using free-atom spectroscopic data to include the promotion energy, going from the atom ground state to the spin configuration in question. Downward-pointing arrows indicate cases where the results are upper bounds on $\Delta E_{\rm coh}$ due to incomplete spectroscopic data. Limitations in the spectroscopic data cause the Os $d^{n-2}sp$ $\Delta E_{\rm coh}$ to be uncertain and, hence, its plotted point has been placed in parentheses.

for the promotion $d^{n-1}s \rightarrow d^n$, i.e., d^n results should lie below $d^{n-1}s$ by about as much as that configuration lies below the $d^{n-2}s^2$ in Fig. 13. Unfortunately, the d^n configuration lies high in energy in the 5*d* elements and as a result is rarely seen. What little data that are available are somewhat questionable, as indicated by the three scattered d^n points on the figure. The d^n configuration is lower lying in the 4*d* row and hence experimentally more accessible. Results that will be reported for the 4*d* row in a future publication *do not* show a $d^{n-1}s \rightarrow d^n$ shift similar to the $d^{n-2}s^2 \rightarrow d^{n-1}s$ shift seen here.

It appears to be the case that the local-density approximation leads to an overestimation of the cohesive energy, as we have seen here. However, Takeuchi and coworkers have obtained[10] a cohesive energy for Au of 3.46 eV/atom with their calculations, which is *smaller* than experiment. This, we believe, is related to their use of pseudopotentials or convergence of their calculation.

VII. CONCLUSIONS

In summary, we have examined the 5*d* row, Hf through Au, with the full-potential LASTO method, which, with its full basis, yields *total energies* to comparable accuracy as other full-potential methods. The ground-state crystal structure is predicted correctly for all the elements using the full potential. Various fine features of the full potential compared to the muffin-tin potential and improvements to the basis have also been examined through numerous plots and tables, with respect to the different crystal structures hcp, fcc, and bcc. Relative lattice stabilities have also been calculated for the above three crystal structures and it is found that the hcp-fcc energy differences are about a factor of 5 smaller in magnitude compared to the fcc-bcc energy differences. The disparity in size in the hcp-fcc energy differences for W and Ta between the estimates of Saunders *et al.*[4] and these and earlier local-density calculations is not expected to change with further refinements in the calculations. We also believe that the disparity will hold when, in the future, we have a better description of the crystal potential than what local-density theory now provides. It seems likely that inclusion of electron-to-atom–ratio (band-filling) effects in the thermodynamic phase-diagram constructs[4] will be necessary to obtain better agreement. The usual overbinding seen in the LDA cohesive energies also occurs for the 5*d*-row elements and some improvements to this problem have also been discussed.

ACKNOWLEDGMENTS

This work was supported by the Division of Materials Sciences of the Office of Basic Energy Sciences, U. S. Department of Energy, under Contract No. DE-AC02-76CH00016.

APPENDIX

The calculations treat the atomic cores self-consistently and fully relativistically, while the bands are treated in the scalar-relativistic approximation, where spin-orbit effects are omitted. The atomic spheres were chosen so that for any given elemental metal the sphere radius is 94.5% of that appropriate to touching atomic spheres in the fcc structure at the observed crystal volume (this choice of radius is equivalent to 97.2% of the touching-sphere radius in the bcc structure at the same volume per atom). This slightly shrunken choice of sphere size was taken in anticipation of calculations for heats of formation of compounds for which the elemental total energies are used as references. It so happens that because of deviations from Vegard's law and because of details of how the atoms are packed in a compound, use of the fcc sphere size in the compounds would cause the spheres to overlap in almost all compounds. Going to this slightly shrunken sphere size allows a large class of compounds to be accommodated without atomic sphere overlapping.

The single set of Slater-type orbitals were taken to be 6*s*-, 6*p*-, and 5*d*-like in character and their screening constants were chosen so as to minimize the crystal total energy, as were the energies at which the scalar-relativistic equations were integrated within the atomic spheres.

Given this set of orbitals, the additional, 7*s*-, 7*p*-, 6*d*-, and 5*f*-like orbitals of the double set had their screening constants optimized. As a rule the 5*f*-like "polarization" orbital provided the greatest benefit to the total energy of the elemental metal, with the 6*d*-like term the next most important. Some examples of the screening constants were given in Ref. 2.

110 special k points were used in the fcc calculations, while 60 and 79 were employed for the hcp and bcc structures, respectively, though in the case of the hcp there are effectively twice the number of k points since there are two atoms in the unit cell.

[1]R. E. Watson, M. Weinert, J. W. Davenport, and G. W. Fernando, Phys. Rev. B **39**, 10 761 (1989).

[2]G. W. Fernando, J. W. Davenport, R. E. Watson, and M. Weinert, Phys. B **40**, 2757 (1989).

[3]*Phase Stability In Metals and Alloys,* edited by P. S. Rudman, J. Stringer, and R. I. Jaffee (McGraw-Hill, New York, 1967).

[4]N. Saunders, A. P. Miodownik, and A. T. Dinsdale, CALPHAD **12**, 351 (1988); see also A. F. Guillermet and M. Hiller, CALPHAD **12**, 337 (1988).

[5]J. W. Davenport, R. E. Watson, and M. Weinert, Phys. Rev. B **32**, 4883 (1985); R. E. Watson, J. W. Davenport, M. Weinert, and L. H. Bennett, in *Thermochemistry of Alloys,* edited by H. Brodowsky and I. Schaller (Kluwer, Dordrecht, The Netherlands, 1989).

[6]For example, H. Skriver, Phys. Rev. B **31**, 1909 (1985); D. Pettifor, CALPHAD **1**, 305 (1977).

[7]J. W. Davenport, Phys. Rev. B **29**, 2896 (1984).

[8]For example, U. von Barth and L. Hedin, J. Phys. C **5**, 1629 (1972).

[9]L. Kaufman and H. Bernstein, *Computer Calculation of Phase Diagrams* (Academic, New York, 1970).

[10]N. Takeuchi, C. T. Chan, and K. M. Ho, Phys. Rev. B **40**, 1565 (1989).

[11]H. J. F. Jansen and A. J. Freeman, Rev. B **30**, 561 (1984).

[12]L. F. Mattheiss and D. R. Hamann, Rev. B **33**, 823 (1986).

[13]C. E. Moore, *Atomic Energy Levels,* U.S. Nat. Bur. Stand. Circ. No. NSRDS-NBS35 (U.S. GPO, Washington, D.C., 1971).

[14]O. Gunnarsson and R. O. Jones, Phys. Rev. B **31**, 7588 (1985).